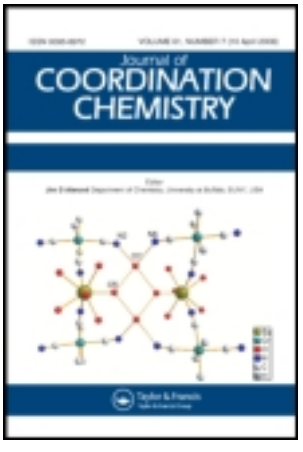

Journal of Coordination Chemistry
Publication details, including instructions for authors and subscription information:
http://www.tandfonline.com/loi/gcoo20

Syntheses, structures, and properties of copper and cadmium complexes with quinoline-based benzimidazole

Yong-Hong Wen [a], Xing-Lei Xie [a] & Lei Wang [a]

[a] Key Laboratory of Eco-chemical Engineering, Ministry of Education, College of Chemistry and Molecular Engineering, Qingdao University of Science and Technology, Qingdao 266042, People's Republic of China

Published online: 10 Jan 2011.

To cite this article: Yong-Hong Wen, Xing-Lei Xie & Lei Wang (2011) Syntheses, structures, and properties of copper and cadmium complexes with quinoline-based benzimidazole, Journal of Coordination Chemistry, 64:3, 459-472, DOI: 10.1080/00958972.2010.548862

To link to this article: http://dx.doi.org/10.1080/00958972.2010.548862

Journal of Coordination Chemistry
Vol. 64, No. 3, 10 February 2011, 459–472

Syntheses, structures, and properties of copper and cadmium complexes with quinoline-based benzimidazole

YONG-HONG WEN*, XING-LEI XIE and LEI WANG

Key Laboratory of Eco-chemical Engineering, Ministry of Education, College of Chemistry and Molecular Engineering, Qingdao University of Science and Technology, Qingdao 266042, People's Republic of China

(*Received 25 September 2010; in final form 3 November 2010*)

A new tridentate ligand 2-((quinolin-8-yloxy)methyl)benzimidazole (**L**) and three coordination compounds, $[CuLCl_2]$ (**1**), $[CuL(H_2O)(SO_4)\cdot 2H_2O]_n$ (**2**), and $\{[Cd_2L_2Cl_4][CdLCl_2(H_2O)]_2\}\cdot H_2O$ (**3**), have been synthesized and characterized. Single crystal structure analyses reveal extensive intermolecular hydrogen bonding, resulting in generation of 1-D–3-D supramolecular networks. Compounds **1** and **2** constitute the first examples of Cu complexes containing both 8-hydroxyquinoline and benzimidazole, while **3** represents the first Cd complex bearing this ligand. Complexes **1**–**3** show similar quasi-reversible electrochemical behaviors. Complex **2** exhibits a predominantly ferromagnetic interaction between copper centers, and **3** has good fluorescence and can be used as an optical material.

Keywords: Copper complex; Cadmium complex; Fluorescence; Electrochemical property; Magnetic property

1. Introduction

Benzimidazole-containing compounds has attracted attention since Hobrecker reported synthesis of the first benzimidazole, 2,5-dimethylbenzimidazole, in 1872 [1, 2]. Investigation of the benzimidazole-containing compound complexes with transition metals is one of the most important subjects in coordination chemistry, crystal engineering, medicine, and material science owing to their fascinating structural motifs [3] and characteristic properties such as luminescence [4, 5], catalysis [6, 7], and antivirus activity [8–10]. Cu complexes $[Cu(SO_4)(pbbm)]_n$ and $\{[Cu(Ac)_2(pbbm)]\cdot CH_3OH\}_n$ (pbbm = 1,1′-(1,5-pentanediyl)*bis*-1*H*-benzimidazole) are efficient homogeneous catalysts for oxidative coupling of 2,6-dimethylphenol [6], while Cu and Cd complexes of several *bis*(benzimidazole) ligands have been examined as potential models of structure and mobility of biological metal binding sites [3].

8-Hydroxyquinoline and its derivatives find wide application in coordination chemistry [11], pharmaceutical chemistry [12–14], and materials chemistry [15]. The syntheses and properties of 8-hydroxyquinoline derivatives and their complexes have

*Corresponding author. Email: yonghwen@163.com

Journal of Coordination Chemistry
ISSN 0095-8972 print/ISSN 1029-0389 online
DOI: 10.1080/00958972.2010.548862

attracted much research [16]. 8-Hydroxyquinoline and benzimidazole are both inexpensive and have large planar π-conjugated systems. However, compounds containing both 8-hydroxyquinoline and benzimidazole have not been investigated. In this article, a new tridentate ligand with N_2O donor set 2-((quinolin-8-yloxy)methyl)benzimidazole (**L**) and three complexes, $[CuLCl_2]$ (**1**), $[CuL(H_2O)(SO_4)\cdot 2H_2O]_n$ (**2**), and $\{[Cd_2L_2Cl_4][CdLCl_2(H_2O)]_2\}\cdot H_2O$ (**3**), have been synthesized and characterized by X-ray diffraction single crystal structure analyses, elemental analyses, infrared (IR) spectra, electrochemical, magnetic, and fluorescence properties.

2. Experimental

2.1. *Materials and measurements*

All commercially available reagents and chemicals were of analytical grade purity and used without purification. Deionized water was obtained by passing distilled water through a Barnstead E-pure 3-Module system. The C, H, and N contents were determined using an Elementar Vario EL III analyzer. IR spectra were recorded from KBr pellets by a Nicolet 510P FT–IR spectrometer. ^{1}H-NMR spectra were recorded by a Bruker Avance 500 MHz spectrometer with TMS as an internal standard. Fluorescence measurements were made on a Hitachi F-4500 fluorescence spectrophotometer.

2.2. *Synthesis*

2.2.1. Synthesis of 2-((quinolin-8-yloxy)methyl)benzimidazole (L). 2-(Quinolin-8-yloxy)acetic acid was synthesized by refluxing an aqueous solution of 8-hydroxyquinoline, 2-chloroacetic acid, and sodium hydroxide for 4 h, followed by acidification with HCl to pH = 2. A mixture of 2-(quinolin-8-yloxy)acetic acid (10.16 g, 0.05 mol), benzene-1,2-diamine (5.41 g, 0.05 mol), and 6 mol L^{-1} HCl (50 mL) was refluxed for 5 h and then cooled to room temperature. The reaction mixture was poured into 200 mL of cold water. A large amount of precipitate appeared when pH was adjusted to 8–9 by adding ammonia dropwise to the mixture. The resulting solid was washed three times with cold water (3×10 mL) to obtain a crude product. Recrystallization of the crude product in C_2H_5OH/CH_3COCH_3 (1 : 1) afforded **L** as colorless crystals. Yield: 9.81 g, 71.3%; m.p.: 179–181°C. ^{1}H-NMR (500 MHz, DMSO-d_6, δ, ppm): 12.84 (s, 1H, NH), 7.20–8.86 (m, 10H, Ph, and py), 5.54 (s, 2H, OCH_2). IR (KBr pellet, cm^{-1}): 3423s, 3286s, 3099m, 3018m, 2896m, 2847m, 2785m, 1619m, 1597w, 1572w, 1546w, 1504s, 1473m, 1459m, 1441s, 1424m, 1354m, 1319s, 1270vs, 1223w, 1116vs, 1088m, 1026w, 827m, 794m, 752vs, 696m, 640w, 590w, 492w, and 437w. Anal. Calcd for $C_{17}H_{13}N_3O$: C, 74.17; H, 4.76; and N, 15.26. Found: C, 74.25; H, 4.69; and N, 15.31.

2.2.2. Synthesis of [CuLCl$_2$] (1). To a methanol solution (10 mL) of **L** (68.8 mg, 0.25 mmol) was added dropwise a methanol solution (5 mL) of $CuCl_2\cdot 2H_2O$ (42.6 mg, 0.25 mmol). The mixture was stirred at room temperature for 5 h and then filtered to

give a clear green solution. Green block crystals suitable for X-ray diffraction analysis of **1** were obtained by slow evaporation of the solvent for 10 days. Yield: 72.7 mg, 71%. IR (KBr pellet, cm^{-1}): 3430s, 3246s, 2922w, 2851w, 1637m, 1624m, 1589w, 1529w, 1506m, 1474m, 1457m, 1446m, 1377m, 1322m, 1264m, 1190w, 1133m, 1072w, 1044w, 1007w, 922w, 823w, 785w, 761m, 742m, 679m, 632m, 563w, 471w, 433w, and 420w. Anal. Calcd for $C_{17}H_{13}Cl_2CuN_3O$: C, 49.83; H, 3.20; and N, 10.25. Found: C, 49.68; H, 3.11; and N, 9.92.

2.2.3. Synthesis of $[CuL(H_2O)(SO_4)\cdot 2H_2O]_n$ (2). To a methanol solution (10 mL) of **L** (68.8 mg, 0.25 mmol) was added dropwise a methanol solution (5 mL) of $CuSO_4\cdot 5H_2O$ (62.4 mg, 0.25 mmol). The mixture was stirred at room temperature for 5 h. The precipitated complex was filtered, washed with methanol, and dried over P_4O_{10} for 48 h. Yield: 91.6 mg, 75%. Blue rhombus crystals suitable for X-ray diffraction analysis of **2** were obtained by slow evaporation of the DMSO/H_2O (3 : 1) solution of the complex for 15 days. IR (KBr pellet, cm^{-1}): 3544vs, 3401s, 3270s, 3059s, 2971s, 2920s, 2848m, 2793m, 1913w, 1871w, 1625w, 1594m 1542w, 1508vs, 1459m, 1444s, 1383w, 1365m, 1326w, 1260vs, 1224s, 1183m, 1127vs, 1055m, 1033m, 1014m, 899w, 851w, 785w, 742vs, 715w, 619w, 600w, and 557w. Anal. Calcd for $C_{17}H_{19}CuN_3O_8S$: C, 41.76; H, 3.92; and N, 8.59. Found: C, 41.69; H, 3.90; and N, 8.52.

2.2.4. Synthesis of $\{[Cd_2L_2Cl_4][CdLCl_2(H_2O)]_2\}\cdot H_2O$ (3). A procedure similar to that described for synthesis of **2** was carried out with **L** (68.8 mg, 0.25 mmol) and $CdCl_2\cdot 2.5H_2O$ (57.1 mg, 0.25 mmol). Yield: 85.0 mg, 70%. Colorless rhombus crystals suitable for X-ray diffraction analysis of **3** were obtained by slow evaporation of the DMSO/H_2O (1 : 1) solution of the complex for 20 days. IR (KBr pellet, cm^{-1}): 3434s, 3283s, 3065w, 2934w, 1621w, 1595w 1584w, 1536w, 1508s, 1473s, 1455m, 1445m, 1379m, 1334m, 1323s, 1265m, 1215w, 1187m, 1128s, 1074w, 1042w, 1017w, 914w, 852w, 824m, 787w, 766m, 748s, 701w, 678m, 622m, 562w, 506w, 463w, and 439w. Anal. Calcd for $C_{68}H_{58}Cd_4Cl_8N_{12}O_7$: C, 43.25; H, 3.10; and N, 8.90. Found: C, 43.30; H, 3.19; and N, 8.82.

2.3. *Electrochemical studies*

All electrochemical experiments were performed with a CHI 832B electrochemical analyzer (Shanghai CHI Instrument Company, China) using a three-electrode system composed of a glassy carbon electrode (GCE, $\varphi = 2.96$ mm) as a working electrode, Ag/AgCl/(saturated)KCl as a reference electrode, and Pt wire as an auxiliary electrode. A 0.2 mol L^{-1} Britton–Robinson buffer solution (BR buffer, the mixture of 3.39 mL 85% H_3PO_4, 2.95 mL HOAc, and 3.0875 g H_3BO_3 was diluted to 250 mL, and adjusted to pH 4.0 with 0.5 mol L^{-1} NaOH) was used. The pH was measured with a PHS-3D pH meter (Shanghai LeiCi Device Works, Shanghai, China) with a combined glass–calomel electrode. Cyclic voltammetry measurements were made on a GCE in BR buffer (pH 4.0) at room temperature with a scan rate of 20–200 mV s^{-1}. The GCE was polished successively with 0.3 and 0.05 μm Al_2O_3 slurry on emery paper. It was then rinsed with doubly distilled water and sonicated in 1 mol L^{-1} HNO_3, acetone and doubly distilled water for 10 min, respectively. The solutions of complexes were

Table 1. Crystal data and structure refinement information of **1**–**3**.

Compounds	**1**	**2**	**3**
Empirical formula	$C_{17}H_{13}Cl_2CuN_3O$	$C_{17}H_{19}CuN_3O_8S$	$C_{68}H_{58}Cd_4Cl_8N_{12}O_7$
Formula weight	409.74	488.95	1888.46
Temperature (K)	113(2)	294(2)	113(2)
Crystal system	Triclinic	Monoclinic	Monoclinic
Space group	$P\bar{1}$	$P2_1/n$	$P2_1/c$
Unit cell dimensions (Å, °)			
a	7.1565(14)	10.7838(19)	19.664(4)
b	9.6969(19)	14.040(2)	12.743(3)
c	12.609(3)	13.344(2)	14.508(3)
α	103.38(3)	90	90
β	105.32(3)	113.39(2)	104.01(3)
γ	103.72(3)	90	90
Volume (Å^3), Z	778.4(3), 2	1854.4(6), 4	3527.1(13), 2
Calculated density (g cm^{-3})	1.748	1.751	1.778
Absorption coefficient, μ (mm^{-1})	1.755	1.346	1.555
Crystal size (mm^3)	$0.10 \times 0.08 \times 0.06$	$0.22 \times 0.20 \times 0.16$	$0.12 \times 0.10 \times 0.04$
θ range for data collection (°)	1.76–25.02	2.07–25.02	1.92–25.02
Reflections collected	4816	9342	19,694
Independent reflections	2735 [R(int) = 0.0332]	3255 [R(int) = 0.0285]	6204 [R(int) = 0.0633]
Data/parameters	2735/217	3255/271	6204/451
Goodness-of-fit on F^2	1.003	1.052	1.157
R^a, wR^b [$I > 2\sigma(I)$]	0.0316, 0.0796	0.0294, 0.0753	0.0604, 0.1479
R^a, wR^b (all data)	0.0388, 0.0828	0.0388, 0.0822	0.0731, 0.1556

$^aR = \Sigma||F_o| - |F_c||/\Sigma|F_o|$. $^bwR = [\Sigma w(F_o^2 - F_c^2)/\Sigma w(F_o^2)^2]^{1/2}$.

prepared by dissolution in an appropriate amount of DMSO and then mixing in BR buffer.

2.4. *Crystal structure determinations*

Single crystal X-ray diffraction data of **1**–**3** were collected on a Bruker SMART 1000 CCD diffactometer with graphite monochromated Mo-Kα radiation ($\lambda = 0.71073$ Å) using ω scan mode at 113(2), 294(2), and 113(2) K, respectively. Intensity data were corrected for *Lp* factors and empirical absorption. The structures were solved by direct methods and refined using full-matrix least-squares on F^2 with SHELXTL program package [17]. The metals were located from the E-map and other non-hydrogen atoms were located with successive difference Fourier syntheses. The hydrogens were generated in ideal positions. Anisotropic thermal parameters were applied to all non-hydrogen atoms. Atomic scattering factors and anomalous dispersion corrections were taken from the International Tables for X-ray Crystallography [18]. Experimental details of the X-ray diffraction analyses of **1**–**3** are given in table 1. Selected bond lengths and angles for **1**–**3** are listed in table 2.

3. Results and discussion

3.1. *Syntheses and general properties*

L was synthesized successfully by simple two-step reactions with 8-hydroxyquinoline as starting material. The synthetic processes gave high yields. The reaction of **L** with metal

Table 2. Selected bond lengths (Å) and angles (°) for **1**–**3**.

Complex **1**			
Cu(1)–N(1)	2.004(2)	Cu(1)–Cl(1)	2.276(2)
Cu(1)–N(2)	1.989(2)	Cu(1)–Cl(2)	2.300(1)
Cu(1)–O(1)	2.228(2)		
O(1)–Cu(1)–Cl(1)	134.70(6)	N(2)–Cu(1)–N(1)	147.68(9)
O(1)–Cu(1)–Cl(2)	100.93(6)	N(2)–Cu(1)–Cl(2)	98.82(7)
Cl(1)–Cu(1)–Cl(2)	124.36(4)	N(1)–Cu(1)–Cl(2)	99.43(8)
Complex **2**			
Cu(1)–N(1)	1.994(2)	Cu(1)–O(2)	2.295(2)
Cu(1)–N(2)	1.963(2)	Cu(1)–O(3A)[a]	2.141(2)
Cu(1)–O(1)	2.151(2)	Cu(1)–O(6)	2.021(2)
N(1)–Cu(1)–O(1)	78.39(7)	N(1)–Cu(1)–O(2)	83.65(8)
N(2)–Cu(1)–O(1)	76.89(7)	N(1)–Cu(1)–O(3A)[a]	88.18(8)
N(1)–Cu(1)–O(6)	103.82(8)	N(2)–Cu(1)–O(2)	89.81(8)
N(2)–Cu(1)–O(6)	100.15(8)	N(2)–Cu(1)–O(3A)[a]	98.78(8)
O(3A)–Cu(1)–O(2)[a]	171.37(8)	O(6)–Cu(1)–O(1)	172.96(8)
Complex **3**			
Cd(1)–N(1)	2.263(5)	Cd(2)–N(4)	2.270(5)
Cd(1)–N(3)	2.322(5)	Cd(2)–N(6)	2.312(6)
Cd(1)–O(1)	2.500(4)	Cd(2)–O(3)	2.481(5)
Cd(1)–O(2)	2.428(4)	Cd(2)–Cl(3)	2.550(2)
Cd(1)–Cl(1)	2.465(2)	Cd(2)–Cl(4)	2.488(2)
Cd(1)–Cl(2)	2.671(2)	Cd(2)–Cl(4A)[b]	2.929(2)
N(1)–Cd(1)–Cl(2)	90.3(1)	N(4)–Cd(2)–O(3)	67.3(2)
N(1)–Cd(1)–O(2)	86.3(2)	N(6)–Cd(2)–O(3)	66.9(2)
N(3)–Cd(1)–Cl(2)	88.8(1)	N(4)–Cd(2)–Cl(4)	120.1(2)
N(3)–Cd(1)–O(2)	83.5(2)	N(6)–Cd(2)–Cl(4)	102.4(1)
Cl(1)–Cd(1)–O(1)	174.1(1)	Cl(3)–Cd(2)–Cl(4A)[b]	172.98(8)
N(3)–Cd(1)–Cl(1)	106.9(1)	N(4)–Cd(2)–Cl(3)	93.9(1)
O(2)–Cd(1)–Cl(1)	94.3(1)	N(6)–Cd(2)–Cl(3)	94.0(1)
N(1)–Cd(1)–Cl(1)	117.4(1)	O(3)–Cd(2)–Cl(3)	93.4(1)
Cl(1)–Cd(1)–Cl(2)	100.09(5)	Cl(4)–Cd(2)–Cl(3)	102.12(8)

Symmetry codes: [a]$x-1/2, -y+1/2, z-1/2$; [b]$-x+1, -y+1, -z$.

salts afforded three different complexes, $[CuLCl_2]$ (**1**), $[CuL(H_2O)(SO_4)\cdot 2H_2O]_n$ (**2**), and $\{[Cd_2L_2Cl_4][CdLCl_2(H_2O)]_2\}\cdot H_2O$ (**3**), depending on the counteranions or on the metal cations in the metal salts. Complex **1** was obtained when $CuCl_2\cdot 2H_2O$ was used, while polynuclear **2** was obtained using $CuSO_4\cdot 5H_2O$; tetranuclear **3** was obtained when $CdCl_2\cdot 2.5H_2O$ was used instead of $CuCl_2\cdot 2H_2O$. All three complexes are stable crystalline solids and can be stored in air at room temperature for a long time. These complexes are soluble in CH_3CN, DMF, and DMSO and slightly soluble in methanol and acetone. IR spectra of ligand and complexes show the N–H characteristic absorptions at 3246–3286 cm^{-1}, indicating that imidazole molecules are coordinated through tertiary nitrogen to metal. This is in agreement with the single crystal structure analyses.

3.2. *Crystal structure of [CuLCl$_2$] (1)*

The molecular structure of **1** is shown in figure 1(a). In **1**, five-coordinate Cu(II) has approximately trigonal bipyramidal geometry. The equatorial positions are occupied by

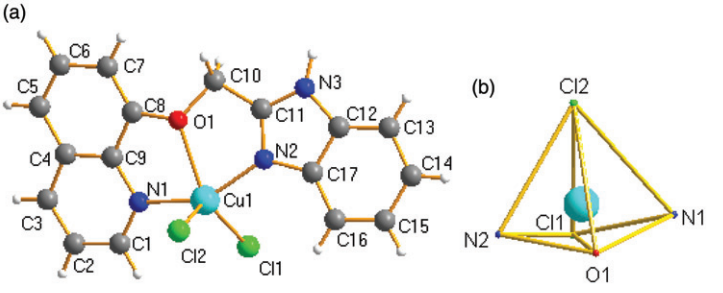

Figure 1. (a) The molecular structure of **1** with the atomic numbering scheme. (b) The coordination polyhedron of Cu^{2+} in **1** with copper deviating from the N_2OCl coordination plane and toward the elongated apical Cl(2).

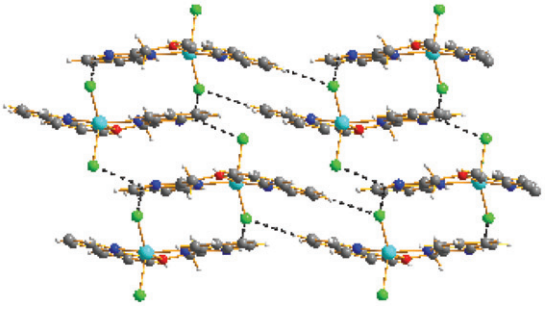

Figure 2. 2-D net structure of **1** along the *b*-axis constructed by hydrogen bonds.

O1 of **L** and two chlorides with the sum of the angles O(1)–Cu(1)–Cl(1), O(1)–Cu(1)–Cl(2), and Cl(1)–Cu(1)–Cl(2) being 359.99°. The axial positions are occupied by two benzimidazole nitrogens with the N(1)–Cu(1)–N(2) angle of 147.68(9)°. The bond lengths, Cu–N 2.004(2) and 1.989(2) Å, Cu–Cl 2.276(2) and 2.300(1) Å, and Cu–O 2.228(2) Å, are within normal ranges for those in similar complexes [3, 19–22]. However, the N(1)–Cu(1)–N(2) angle of 147.68(9)° deviates from the "ideal" value of 180° [23] and the trigonality index τ of 0.22 is close to the τ value of zero for a perfect square pyramidal [24], so the coordination geometry around copper is intermediate between trigonal bipyramidal and square pyramidal geometries and is best described as trigonal bipyramidal distorted square-based pyramidal [20, 21] with copper displaced 0.639 Å above the N_2OCl coordination plane and toward the elongated apical Cl(2) (figure 1b). The dihedral angle between quinoline and benzimidazole rings in **1** is 14.12(9)°.

There exist different types of hydrogen bonds in **1**. Intermolecular N(3)–H(3A)···Cl(1) hydrogen bonds connect the complex into a head-to-tail dimer $[CuLCl_2]_2$. Intermolecular N(3)–H(3A)···Cl(2) hydrogen bonds connect dimers into 1-D chain structures constructed by $[CuLCl_2]_2$ as building unit. Finally, these 1-D chain structures are linked by intermolecular C(2)–H(2)···Cl(1) hydrogen bonds forming a 2-D net structure (figure 2). In **1**, there are two types of bifurcated hydrogen bonds: N(3)–H(3A)···Cl(1)/Cl(2), where H(3A) was shared by Cl(1) and Cl(2) to form a tricentered hydrogen bond, and N(3)–H(3A)/C(2)–H(2)···Cl(1), two donors H(3A)

Table 3. Hydrogen bond data (Å) and (°) for **1**–**3**.

D–H···A	*d*(D–H)	*d*(H···A)	*d*(D···A)	∠DHA
Complex **1**				
N(3)–H(3A)···Cl(1)[a]	0.90	2.58	3.227(2)	129.4
N(3)–H(3A)···Cl(2)[b]	0.90	2.69	3.341(3)	130.1
C(2)–H(2)···Cl(1)[c]	0.93	2.82	3.749(3)	177.2
Complex **2**				
O(6)–H(6A)···O(5)	0.85	1.88	2.714(3)	164.9
O(6)–H(6B)···O(7)[d]	0.86	1.83	2.681(3)	170.1
N(3)–H(3A)···O(4)[e]	0.89	1.80	2.690(3)	179.0
O(7)–H(7A)···O(8)[f]	0.85	2.03	2.852(4)	164.1
O(7)–H(7B)···O(5)[g]	0.85	1.96	2.813(3)	171.6
O(8)–H(8A)···O(4)[h]	0.86	1.92	2.749(3)	162.8
C(3)–H(3)···O(2)[h]	0.93	2.52	3.356(3)	149.0
C(7)–H(7)···O(7)	0.93	2.43	3.343(4)	166.1
Complex **3**				
O(2)–H(2B)···Cl(2)[i]	0.85	2.78	3.230(4)	114.9
N(2)–H(2C)···Cl(2)[j]	0.86	2.35	3.178(6)	160.7
O(4)–H(4A)···N(5)[k]	0.86	2.54	3.302(10)	148.0
O(4)–H(4A)···Cl(3)[l]	0.86	2.75	3.302(11)	123.0
N(5)–H(5A)···Cl(3)[m]	0.86	2.64	3.346(8)	140.7
C(29)–H(29)···Cl(1)[n]	0.93	2.74	3.666(8)	174.0

Symmetry codes: [a] $-x+1, -y+1, -z+1$; [b] $-x+2, -y+1, -z+1$; [c] $-x+1, -y+1, -z+2$; [d] $x+1/2, -y+1/2, z-1/2$; [e] $-x+3/2, y+1/2, -z+3/2$; [f] $-x+1/2, y+1/2, -z+3/2$; [g] $x-1, y, z$; [h] $-x+3/2, y-1/2, -z+3/2$; [i] $x, -y+1/2, z+1/2$; [j] $-x+2, y-1/2, -z+1/2$; [k] $-x+1, -y, -z+1$; [l] $x, -y+1/2, z+1/2$; [m] $-x+1, y-1/2, -z+1/2$; [n] $-x+2, -y+1, -z+1$.

and H(2) share one acceptor Cl(1) to form another tricentered hydrogen bond. Hydrogen bond data are shown in table 3. In addition, the crystal packing exhibits π–π stacking interactions. The short centroid–centroid distances between the imidazole rings of the neighboring molecules are 3.396(2) Å, and those between pyridine and benzene rings in quinoline of the neighboring molecules 3.691(2) Å.

3.3. *Crystal structure of* $[CuL(H_2O)(SO_4)\cdot 2H_2O]_n$ *(2)*

The molecular structure of **2** is shown in figure 3. In **2**, each Cu(II) is six-coordinate by two nitrogens from **L** and four oxygens, one from **L**, one from a crystal water, and two from two different sulfates. All coordinated bond lengths show normal values and are comparable to those in **1** and in the other related compounds [3, 19–22]. The coordination geometry around Cu is best described as octahedral. The equatorial positions are occupied by O(1), O(6), N(1), and N(2) with the sum of the angles N(1)–Cu(1)–O(1), N(2)–Cu(1)–O(1), N(1)–Cu(1)–O(6), and N(2)–Cu(1)–O(6) being 359.25°, and the axial positions by O(2) and O(3A) with O(2)–Cu(1)–O(3A) angle being 171.36(8)°. The dihedral angle between quinoline ring and benzimidazole ring is 10.41(8)° in **2**. Complex **2** is linked by bridging bidentate sulfates to form a 1-D infinite chain (figure 4a). The distance of two neighboring Cu's in the chain is 6.718 Å, while the distances of two neighboring Cu's between the chains are 7.886 Å and 8.727 Å. The 1-D chains are connected by short aromatic ring π–π stacking (figure 4a) and intermolecular hydrogen bond interactions (figure 4b) to form a 3-D supramolecular structure. The distances between aromatic rings in neighboring molecules are from 3.307 to 3.446 Å.

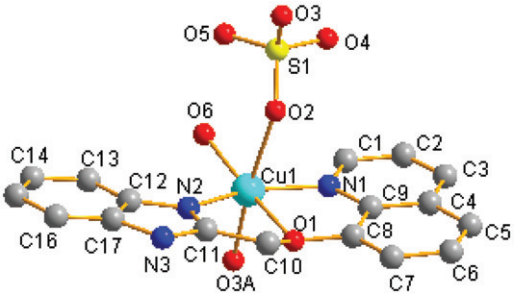

Figure 3. The molecular structure of **2** showing the atom labeling scheme. Hydrogens are omitted for clarity. O3A is related to O3 by the symmetry operator $(x-1/2, -y+1/2, z-1/2)$.

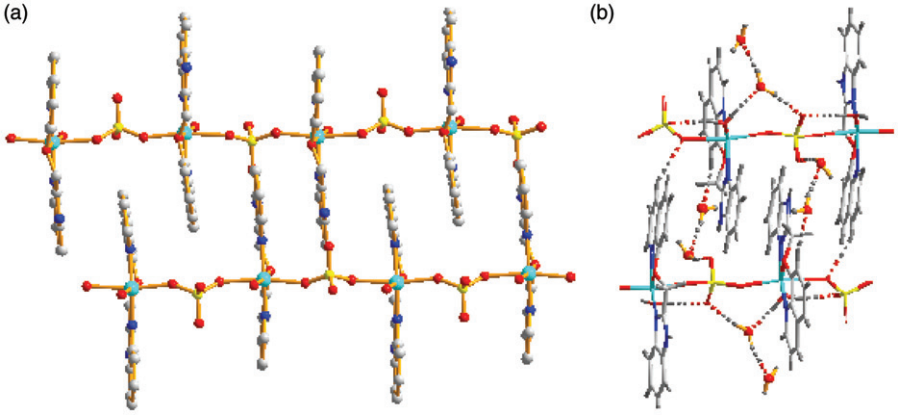

Figure 4. (a) The 1-D infinite chain structure of **2** showing the π–π stacking interactions among the aromatic rings. The hydrogens and solvent molecules are omitted for clarity. (b) The hydrogen bond interactions between the 1-D chains in **2**. Waters are shown in ball and stick style, and the hydrogen bonds are shown as dashed lines for clarity.

Three types of hydrogen bonds are found in **2**: namely, O–H···O (O···O = 2.681(3)–2.852(4) Å), N–H···O (N···O = 2.690(3) Å), and C–H···O (C···O = 3.343(4)–3.356(3) Å) (table 3).

3.4. *Crystal structure of* $\{[Cd_2L_2Cl_4][CdLCl_2(H_2O)]_2\}\cdot H_2O$ *(3)*

The asymmetric unit of **3** contains one half-molecule, the other half being related by a crystallographic center of symmetry (figure 5), except for the uncoordinated crystal water because the site occupancy factors of all atoms in the crystal water are 0.5. There exist two different kinds of cadmium(II) in **3**. Cd(1) is six-coordinate by two nitrogens from **L**, two chlorides and two oxygens, one from **L**, and another from water. The coordination geometry around Cd(1) is an approximate octahedron. The equatorial positions are occupied by N(1), O(2), N(3), and Cl(2) with the sum of the angles Cl(2)–Cd(1)–N(1), O(2)–Cd(1)–N(1), Cl(2)–Cd(1)–N(3), and O(2)–Cd(1)–N(3)

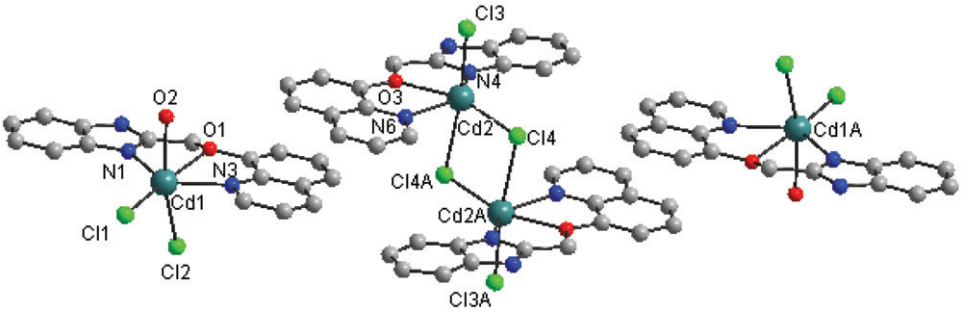

Figure 5. The molecular structure of **3** showing the main atom labeling scheme. The hydrogens and crystal water are omitted for clarity. The suffix A corresponds to symmetry code $(-x+1, -y+1, -z)$.

being 348.88°, and the axial positions by Cl(1) and O(1) with the angle of O(1)–Cd(1)–Cl(1) being 174.06° and the distances of Cd(1)–O(1) and Cd(1)–Cl(1) 2.500(4) and 2.464(2) Å, respectively. The Cd(1) is displaced 0.597 Å above the N_2OCl coordination plane and toward the apical Cl(1), due to steric hindrance formed by two chelate rings. Cd(1)–Cl(2) length of 2.672(2) Å is the longest of the six-coordinate bond lengths, attributed to formation of intermolecular hydrogen bonds by Cl(2) to O(2) and N(2) of neighboring molecules. The Cd(2) is also six-coordinate, similar to that of Cd(1) with the coordinated water being replaced by a bridging Cl(4A). The Cl(4) also bridges another Cd(2A) to form a dinuclear complex $[Cd_2L_2Cl_4]$. The separation of two bridging Cd(2)'s in the dinuclear complex is 4.016 Å. Because of the bridging coordination, the Cd(2)–Cl(4A) distance (and Cd(2A)–Cl(4)) reaches 2.929(2) Å, the longest in **3**, but still comparable with those in the related complexes [25–27].

The ligand molecules in both Cd(1) and Cd(2) in **3** are almost coplanar, as indicated by dihedral angles between quinoline and benzimidazole rings of 2.61(2)° and 5.78(2)°, respectively. Each benzimidazolyl in the Cd(1) complex has π–π stacking interaction with another benzimidazolyl from the adjacent Cd(1) unit. The distance between the stacked planes is 3.299 Å. The Cd(1) and Cd(2) complexes are connected by intermolecular C(29)–H(29)···Cl(1) hydrogen bond [C···Cl = 3.666(8) Å]. A hydrogen of coordinated water in the Cd(1) unit is hydrogen bonded to two chlorides from two neighboring Cd(1) complexes [O(2)···Cl(2) = 3.230(4) Å and O(2)···Cl(1) = 3.208(4) Å]; Cl(2) also has a hydrogen bond interaction with H–N of another Cd(1) complex [N(2)···Cl(2) = 3.178(6) Å]. In addition, a hydrogen of benzimidazole in the Cd(2) complex is hydrogen bonded to Cl(3) of the neighboring Cd(2) complex [N(5)···Cl3 = 3.346(8) Å]. These hydrogen bonds and the π–π stacking interactions link **3** to form a 3-D supramolecular structure.

3.5. *Electrochemical behaviors of 1–3*

Electrochemical behaviors of **1**–**3** were studied by measuring their cyclic voltammograms in 5 mL of 0.2 mol·L^{-1} BR buffer solution (pH 4.0) containing 1.0×10^{-4} mol L^{-1} complexes. As shown in figure 6(a), **1** shows a pair of redox peaks with a cathodic peak potential (E_{pc}) at 0.124 V and an anodic peak potential (E_{pa}) at 0.325 V. The formal potential ($E_{1/2} = 1/2(E_{pa} + E_{pc})$) and the peak-to-peak potential

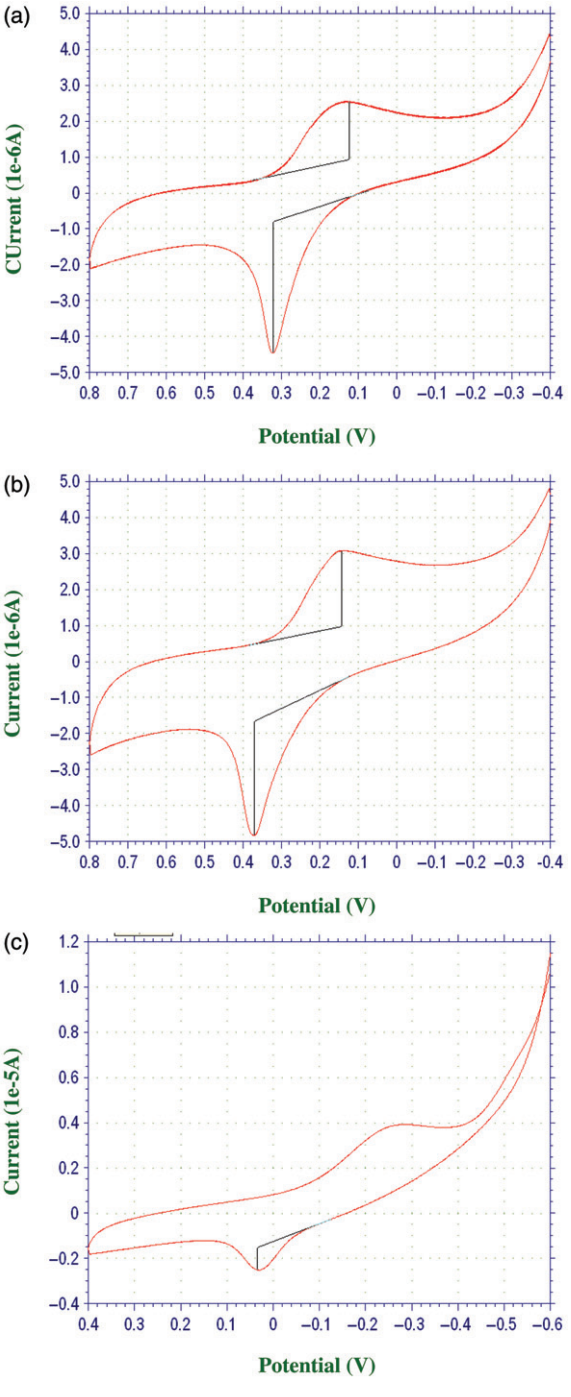

Figure 6. Cyclic voltammograms of (a) **1**, (b) **2**, and (c) **3** in 5 mL 0.2 mol L^{-1} BR buffer (pH 4.0). Complex concentration: 1.0×10^{-4} mol L^{-1}. Scan rate: 100 mV s^{-1}.

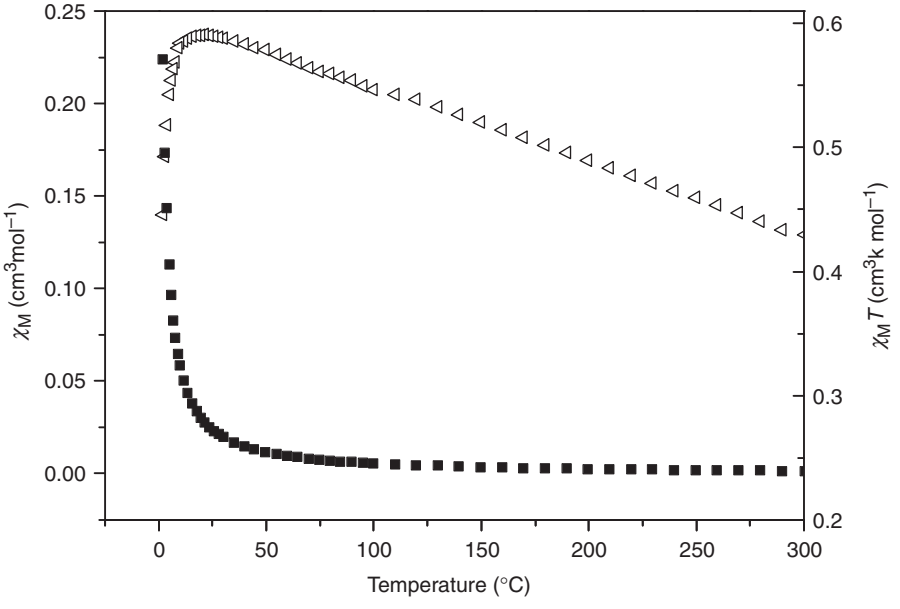

Figure 7. χ_M *vs.* T (■) and $\chi_M T$ *vs.* T (Δ) plots of **2**.

separation (ΔE_p) were obtained as 0.225 V and 0.201 V, respectively, indicating that the electrochemical behavior of **1** is quasi-reversible corresponding to $Cu(II) + e \leftrightarrow Cu(I)$ [28–30]. Similarly, **2** shows a quasi-reversible one-electron redox at $E_{1/2} = 0.257$ V corresponding to the electrode process $Cu(II) + e \leftrightarrow Cu(I)$, with E_{pc} at 0.147 V and E_{pa} at 0.367 V (figure 6b); **3** shows a quasi-reversible two-electron redox process at $E_{1/2} = -0.123$ V corresponding to $Cd(II) + 2e \leftrightarrow Cd(0)$, with $E_{pc} = -0.279$ V, $E_{pa} = 0.034$ V and $i_{pc}/i_{pa} = 4.028$ (figure 6c) [31, 32].

3.6. *Magnetic property of 2*

Temperature dependence of the magnetic susceptibility of **2** was investigated in the temperature range 4–300 K at 2 KOe (figure 7). The $\chi_M T$ *versus* T plot exhibits a value of 0.43 emu K Oe^{-1} mol^{-1} at 300 K and continuously increases on cooling to a value of 0.61 emu K Oe^{-1} mol^{-1} at 24 K. This behavior of the $\chi_M T$ curve shows ferromagnetic interactions in **2**. However, the curve drops abruptly below 14 K, indicating that an antiferromagnetic interaction exists in **2** at lower temperatures. The effective magnetic moment (1.85 μ_B per Cu) at 300 K is in good agreement with the theoretical value (1.73 μ_B) for an uncoupled copper ion, calculated from $\mu_{eff} = 2.828(\chi_M T)^{1/2}$. The Weiss constant, determined in the temperature range 4–300 K, is 8.49 K, suggesting a predominantly ferromagnetic interaction between the copper centers. According to the structural data, the Cu···Cu distance in the 1-D chains (6.7177 Å) bridged by the SO_4^{2-} can contribute to the ferromagnetic interaction.

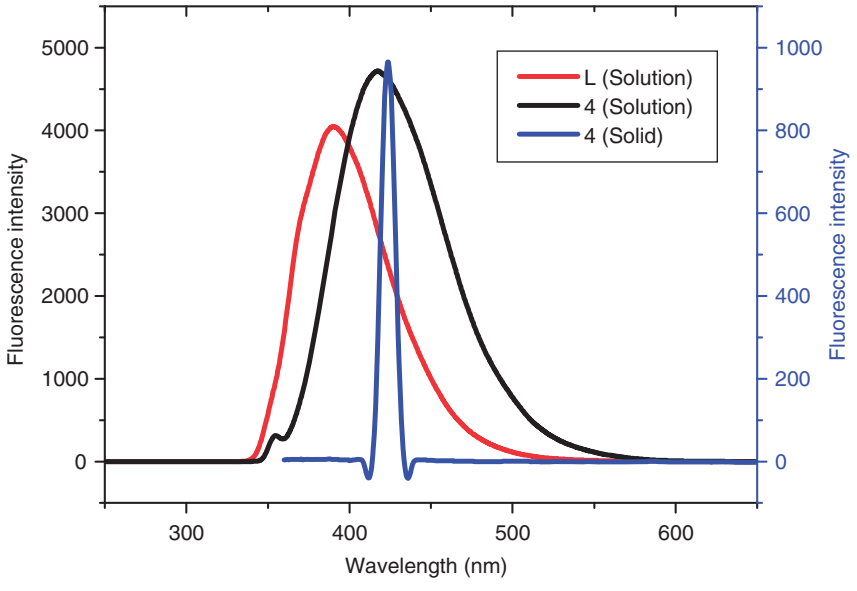

Figure 8. Fluorescence spectra of **L** (red) and **3** (black) in DMSO–water solution, and **3** (blue) in solid state at room temperature. Compound concentration in solution: **L**, 4.0×10^{-3} mol L^{-1} and **3**, 1.0×10^{-3} mol L^{-1}.

3.7. *Fluorescent properties*

Emission spectra of **L** and **3** at room temperature are shown in figure 8. In DMSO–water, free **L** displays an intense fluorescence emission maximum at 390.2 nm when excited at 340 nm, assigned to the intraligand (π–π*) fluorescent emission. In the same conditions, **3** exhibits more intense fluorescence with an emission maximum at 417.2 nm upon excitation at 350 nm, red-shifted 27 nm. The enhancement of fluorescence in **3** with d^{10} configuration may be attributed to the chelating coordination of the ligand to the cadmium [33]. The coordination increases the rigidity of the ligand, as indicated in X-ray diffraction analysis, and thus reduces the loss of energy through a radiationless pathway. The significant red shift of the emission in **3** is attributed to ligand-to-metal charge transfer, which has been found in similar Cd coordination compounds [34–36]. The fluorescence of **3** in the solid state at room temperature was also studied, as depicted in figure 8. The solid complex **3** exhibits a purple/blue narrow emission band (bandwidth at half-height 10 nm) with maximum at 424 nm when excited at 380 nm, suggesting **3** can be used as an optical material.

4. Conclusion

A new tridentate ligand 2-((quinolin-8-yloxy)methyl)benzimidazole and its three coordination compounds have been prepared and structurally characterized. The formation of different complexes depends both on the counteranions and on the metal cations. In the complexes, **L** adopts the same coordination and essentially planar conformation. The electrochemical properties of the complexes show potential for

further applications in electrochemical sensors or electroanalysis. The magnetic and fluorescent properties suggest the compounds could have potential as ferromagnetic or fluorescent materials. In view of the flexibility, rigidity, and large planar configuration with π-conjugated system of 2-((quinolin-8-yloxy)methyl)benzimidazole, it is possible to prepare novel complexes with interesting chemical and physical properties.

Supplementary material

Crystallographic data for the structural analysis of the compounds has been deposited with the Cambridge Crystallographic Data Center (CCDC). CCDC reference numbers 776437–776439 contain the supplementary crystallographic data for this article. These data can be obtained free of charge from The Cambridge Crystallographic Data Centre *via* www.ccdc.cam.ac.uk/data_request/cif.

Acknowledgments

This work was supported by the National Natural Science Foundation of China (no. 20971076), the Outstanding Adult-Young Scientific Research Encouraging Foundation of Shandong Province, China (no. 2008BS09017).

References

[1] F. Hobrecker. *Ber*., **5**, 920 (1872).
[2] J.B. Wright. *Chem. Rev*., **48**, 397 (1951).
[3] J.C. Lockhart, W. Clegg, M.N.S. Hill, D.J. Rushton. *J. Chem. Soc., Dalton Trans*., 3541 (1990).
[4] Q.-D. Liu, W.-L. Jia, S. Wang. *Inorg. Chem*., **44**, 1332 (2005).
[5] Y. Wang, H.-B. Xu, Z.-M. Su, K.-Z. Shao, Y.-H. Zhao, H.-P. Cui, Y.-Q. Lan, X.-R. Hao. *Inorg. Chem. Commun*., **9**, 1207 (2006).
[6] B. Xiao, H. Hou, Y.J. Fan. *Organomet. Chem*., **692**, 2014 (2007).
[7] W.-D. Chen, S.-R. Zhu, H.-K. Lin. *Chem. Res. Chin. Univ*., **18**, 1321 (1997).
[8] W.R. Roderick, J.C.W. Nordeen, A.M. von Esch, R.N. Appell. *J. Med. Chem*., **15**, 655 (1972).
[9] N.M. Salunke, V.K. Revankar, V.B. Mahale. *Transition Met. Chem*., **19**, 53 (1994).
[10] Y.-F. Li, G.-F. Wang, P.-L. He, W.-G. Huang, F.-H. Zhu, H.-Y. Gao, W. Tang, Y. Luo, C.-L. Feng, L.-P. Shi, Y.-D. Ren, W. Lu, J.-P. Zuo. *J. Med. Chem*., **49**, 4790 (2006).
[11] W.G. Hanna, M.M. Moawad. *J. Coord. Chem*., **55**, 43 (2002).
[12] J.-L. Pierre, P. Baret, G. Serratrice. *Curr. Med. Chem*., **10**, 1077 (2003).
[13] A.K. Patel, V.M. Patel. *Synth. React. Inorg. Met.-Org. Chem*., **29**, 193 (1999).
[14] N. Muruganantham, R. Sivakumar, N. Anbalagan, V. Gunasekaran, J.T. Leonard. *Biol. Pharm. Bull*., **27**, 1683 (2004).
[15] C.W. Tang, S.A. VanSlyke. *Appl. Phys. Lett*., **51**, 913 (1987).
[16] H.-P. Zeng, X.-H. OuYang, T.-T. Wang, G.-Z. Yuan, G.-H. Zhang, X.-M. Zhang. *Cryst. Growth Des*., **6**, 1697 (2006).
[17] G.M. Sheldrick. *SHELXTL 6.10*, Bruker Analytical Instrumentation, Madison, Wisconsin, USA (2000).
[18] A.J.C. Wilson. *International Tables for X-ray Crystallography*, Vol. C, Kluwer Academic Publishers, Dordrecht (1992), Tables 6.1.1.4 (pp. 500–520) and 4.2.6.8 (pp. 219–222), respectively.
[19] M.R.A. Al-Mandhary, P.J. Steel. *Inorg. Chim. Acta*, **351**, 7 (2003).
[20] C.J. Matthews, T.A. Leese, W. Clegg, M.R.J. Elsegood, L. Horsburgh, J.C. Lockhart. *Inorg. Chem*., **35**, 7563 (1996).

[21] M. Vaidyanathan, R. Balamurugan, U. Sivagnanam, M. Palaniandavar. *J. Chem. Soc., Dalton Trans.*, 3498 (2001).
[22] Y.-T. Cheng, H.-L. Chen, S.-Y. Tsai, C.-C. Su, H.-S. Tsang, T.-S. Kuo, Y.-C. Tsai, F.-L. Liao, S.-L. Wang. *Eur. J. Inorg. Chem.*, 2180 (2004).
[23] J.V. Dagdigian, V. McKee, W. Clegg, C.A. Reed. *Inorg. Chem.*, **21**, 1332 (1982).
[24] A.W. Addison, T.N. Rao, J. Reedijk, J. van Rijn, G.C. Verschoor. *J. Chem. Soc., Dalton Trans.*, 1349 (1984).
[25] C.J. Matthews, W. Clegg, S.L. Heath, N.C. Martin, M.N.S. Hill, J.C. Lockhart. *Inorg. Chem.*, **37**, 199 (1998).
[26] L.-F. Zu, Y. Wang, Z.-M. Su, K.-Z. Shao, Y.-H. Zhao. *Acta Crystallogr.*, **E63**, m292 (2007).
[27] C.-K. Xia, Q.-Z. Zhang, S.-M. Chen, X. He, C.-Z. Lu. *Acta Crystallogr.*, **C61**, m203 (2005).
[28] R. Balamurugan, M. Palaniandavar, R.S. Gopalan. *Inorg. Chem.*, **40**, 2246 (2001).
[29] H. Nagao, N. Komeda, M. Mukaida, M. Suzuki, K. Tanaka. *Inorg. Chem.*, **35**, 6809 (1996).
[30] J.A. Guckert, M.D. Lowery, E.I. Solomon. *J. Am. Chem. Soc.*, **117**, 2817 (1995).
[31] W. Li, C.-H. Li, Y.-Q. Yang, Z.-M. Chen, Y. Wang. *Chin. J. Inorg. Chem.*, **24**, 1360 (2008).
[32] R.T. Stibrany, M.V. Lobanov, H.J. Schugar, J.A. Potenza. *Inorg. Chem.*, **43**, 1472 (2004).
[33] L.-Y. Zhang, J.-P. Zhang, Y.-Y. Lin, X.-M. Chen. *Cryst. Growth Des.*, **6**, 1684 (2006).
[34] Z.W. Wang, C.C. Ji, J. Ji, Z.J. Guo, Y.Z. Li, H.G. Zheng. *Cryst. Growth Des.*, **9**, 475 (2009).
[35] W.-G. Lu, L. Jiang, X.-L. Feng, T.-B. Lu. *Cryst. Growth Des.*, **6**, 564 (2006).
[36] R. Wang, D. Yuan, F. Jiang, L. Han, Y. Gong, M. Hong. *Cryst. Growth Des.*, **6**, 1351 (2006).